

## Excitonic and Valley-Polarization Signatures of Fractional Correlated Electronic Phases in a WSe<sub>2</sub>/WS<sub>2</sub> Moiré Superlattice

Erfu Liu<sup>1</sup>, Takashi Taniguchi,<sup>2</sup> Kenji Watanabe,<sup>3</sup> Nathaniel M. Gabor,<sup>1,4</sup> Yong-Tao Cui,<sup>1</sup> and Chun Hung Lui<sup>1,\*</sup>

<sup>1</sup>*Department of Physics and Astronomy, University of California, Riverside, California 92521, USA*

<sup>2</sup>*International Center for Materials Nanoarchitectonics (WPI-MANA), National Institute for Materials Science (NIMS), 1-1 Namiki Tsukuba, Ibaraki 305-0044, Japan*

<sup>3</sup>*National Institute for Materials Science (NIMS), 1-1 Namiki Tsukuba, Ibaraki 305-0044, Japan*

<sup>4</sup>*Canadian Institute for Advanced Research, MaRS Centre West Tower, 661 University Avenue, Toronto, Ontario ON M5G 1M1, Canada*



(Received 7 January 2021; accepted 27 May 2021; published 16 July 2021)

We have measured the reflectance contrast, photoluminescence, and valley polarization of a WSe<sub>2</sub>/WS<sub>2</sub> heterobilayer moiré superlattice at gate-tunable charge density. We observe absorption modulation of three intralayer moiré excitons at filling factors  $\nu = 1/3$  and  $2/3$ . We also observe luminescence modulation of interlayer trions at around a dozen fractional filling factors, including  $\nu = -3/2, 1/4, 1/3, 2/5, 2/3, 6/7, 5/3$ . Remarkably, the valley polarization of interlayer trions is suppressed at some fractional fillings. These results demonstrate that electron crystallization can modulate the absorption, emission, and valley dynamics of the excitonic states in a moiré superlattice.

DOI: [10.1103/PhysRevLett.127.037402](https://doi.org/10.1103/PhysRevLett.127.037402)

Two-dimensional (2D) moiré superlattices have recently opened a fertile new ground to explore strongly correlated quantum phases, including Mott insulators, superconductors, and correlated magnetic phases [1–15]. In particular, moiré superlattices formed by two monolayers of transition metal dichalcogenides (TMDs) can exhibit correlated insulating states at fractional fillings [2,16–22]. In these superlattices, the Coulomb interactions are markedly enhanced by the 2D confinement, yet the carrier kinetic energy is strongly suppressed by the large carrier effective mass and slow hopping between moiré cells. As a result, electrons tend to distribute themselves in an orderly fashion to reduce their total energy, leading to crystalline electron phases. Recent research has reported evidence of generalized Wigner crystals and stripe phases at fractional fillings of WSe<sub>2</sub>/WS<sub>2</sub> heterobilayer moiré superlattices from their dielectric, capacitance, and optical response [2,16–19].

With the initial experiments focusing on the capacitance and dielectric response of fractional correlated electronic phases, there is currently a lack of studies on how the fractional correlated electronic phases affect the excitonic and valleytronic properties of the materials. Moiré superlattices formed by valley semiconductors (e.g., MoS<sub>2</sub>, WSe<sub>2</sub>, and WS<sub>2</sub>) are known to host robust excitonic states with distinctive valleytronic properties, which hold promises for novel excitonic and valleytronic applications [23–32]. The coupling between these valley excitonic states and the crystalline electron phases may enable new methods to control the properties of van der Waals heterostructures. Therefore, it is intriguing to explore excitonic phenomena in the regime of electron crystallization.

In this Letter, we report the observation of excitonic and valley-polarization signatures of correlated electronic phases at fractional fillings in a WSe<sub>2</sub>/WS<sub>2</sub> moiré superlattice. We observe significant absorption modulation of three WSe<sub>2</sub> intralayer moiré excitons at fractional fillings  $\nu = 1/3$  and  $2/3$ . The higher-lying moiré excitons are more sensitive to the fractional correlated phases than the lower-lying moiré excitons. We also observe abrupt changes in the photoluminescence (PL) intensity and photon energy of the interlayer trions at a series of fractional fillings, including  $\nu = -3/2, 1/4, 1/3, 2/5, 2/3, 6/7, 5/3$ . Remarkably, the valley polarization of interlayer trions decreases noticeably at some fractional fillings. Therefore, the absorption, emission, and valley dynamics of the excitonic states all change significantly at fractional fillings.

Our WSe<sub>2</sub>/WS<sub>2</sub> heterobilayers are formed by stacking monolayer WSe<sub>2</sub> and monolayer WS<sub>2</sub> with a nearly 60° interlayer rotation angle. Because of the ~4% mismatch between the WSe<sub>2</sub> and WS<sub>2</sub> lattice constants, the heterobilayer can exhibit a moiré pattern with a period of ~8 nm [Fig. 1(a)]. An electron (hole) density  $n \sim 1.8 \times 10^{12} \text{ cm}^{-2}$  can fill one electron (hole) per moiré cell, corresponding to the filling factor  $\nu = +1$  ( $-1$ ). The heterobilayer is encapsulated by hexagonal boron nitride (BN) and equipped with top and bottom gates with thin graphite as electrodes [Fig. 1(b)] [33]. We measure the reflectance contrast and PL, which reveal the absorption and emission properties of the superlattice, respectively [33]. We have measured several devices and here present the results of the best device (device 1) (see the Supplemental Material for the results of two other devices [33]). The device exhibits

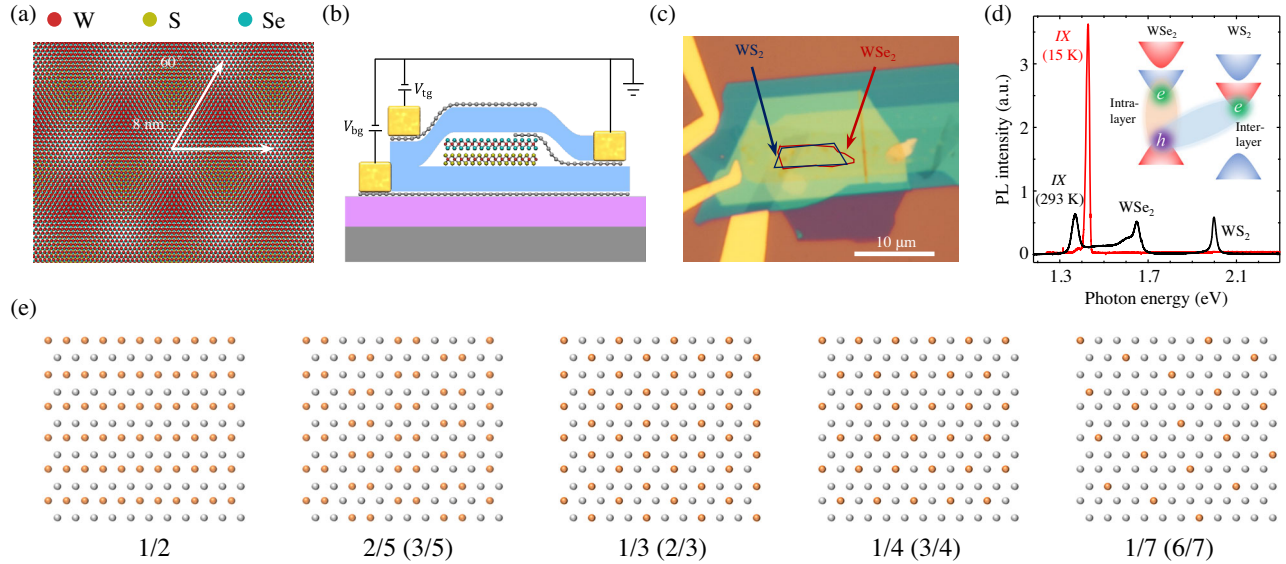


FIG. 1. (a) Moiré pattern in the  $\text{WSe}_2/\text{WS}_2$  heterobilayer with a  $60^\circ$  interlayer rotation angle. (b),(c) Schematic and optical image of our  $\text{WSe}_2/\text{WS}_2$  heterobilayer device. (d) Photoluminescence spectra at  $T \sim 15$  K, 293 K under 532-nm laser excitation. We denote emission peaks from intralayer  $\text{WSe}_2$  excitons, intralayer  $\text{WS}_2$  excitons, and interlayer excitons (IX). The inset shows the band configurations of intralayer and interlayer excitons. The band color represents different electron spins. (e) Schematic charge distributions of possible correlated electronic phases at different fractional fillings in the moiré superlattice. The orange (silver) dots represent moiré cells filled (unfilled) with an electron. Exchanging the orange and silver color gives configurations with complementary filling factors denoted in the parentheses.

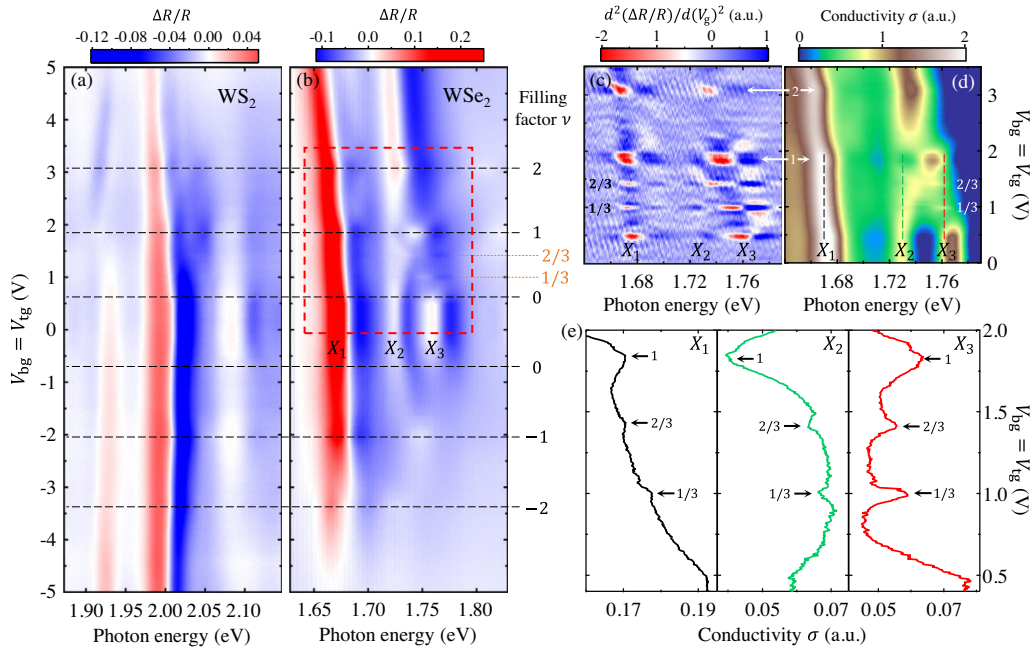


FIG. 2. (a), (b) Gate-dependent reflectance contrast maps for the intralayer excitonic states within the  $\text{WS}_2$  layer and  $\text{WSe}_2$  layer in the  $\text{WSe}_2/\text{WS}_2$  moiré superlattice at temperature  $T \sim 15$  K. We inject electrons (holes) by applying an equal positive (negative) voltage ( $V_g$ ) on the back gate ( $V_{bg}$ ) and top gate ( $V_{tg}$ ). The dashed lines denote the integer and fractional filling positions. The zero filling lines correspond approximately to the boundary of the charge neutral region. (c) Second-order gate-voltage ( $V_g$ ) derivative of a finely scanned reflectance contrast map within the red dashed box in panel (b). (d) The extracted real part of the optical sheet conductivity ( $\sigma$ ) of the heterobilayer within the region of the red dashed box in panel (b). (e) Conductivity profiles along the three dashed lines with the corresponding color in panel (d).

significant interlayer exciton PL even at room temperature, indicating high device quality [Figs. 1(c) and 1(d)].

Figures 2(a) and 2(b) display the gate-dependent reflectance contrast ( $\Delta R/R$ ) maps at temperature  $T \sim 15$  K. In the charge neutrality regime (gate voltage  $V_g \sim 0$ ), we observe two  $\text{WS}_2$  intralayer moiré excitons near photon energies 1.991 and 2.082 eV [Fig. 2(a)] as well as three  $\text{WSe}_2$  intralayer moiré excitons near 1.672, 1.724, and 1.76 eV [Fig. 2(b); labeled as  $X_1$ ,  $X_2$ , and  $X_3$ , respectively]. The emergence of moiré excitons indicates a substantial influence of the moiré superlattice on the excitonic states, as shown in prior studies [16,24,28,29]. As the top and bottom gates of our device have nearly the same BN thickness ( $\sim 25$  nm), we can inject electrons (holes) into the heterobilayer without inducing a vertical electric field by applying equal positive (negative) gate voltage on the bottom gate ( $V_{\text{bg}}$ ) and top gate ( $V_{\text{tg}}$ ). From the hole to electron side, we observe spectral modulation of moiré excitons at  $V_g = V_{\text{bg}} = V_{\text{tg}} = -3.34, -2.02, 1.86, 3.08$  V. They correspond to integer fillings  $\nu = -2, -1, 1, 2$ , respectively, according to our estimated charge density and comparison with prior studies [2,3,16,18]. Here

$\nu = \pm 2 (\pm 1)$  correspond to complete (half) filling of a moiré miniband [2,3]. The spectral changes at  $\nu = \pm 1$  signify the formation of a Mott phase [2,3] or charge-transfer phase [38] at half filling.

Remarkably, the  $\text{WSe}_2$  moiré excitons exhibit spectral modulation at  $\nu = 1/3, 2/3$  in the red dashed box in Fig. 2(b). We have finely scanned this region and performed second-order gate-voltage derivative to sharpen the relevant spectral modulation [Fig. 2(c)]. From the reflectance contrast, we further extract the real part of the optical conductivity of the heterobilayer by Kramer-Kronig constrained variational analysis [Fig. 2(d)] [33,36]. The gate-dependent conductivity profiles of  $X_1, X_2$ , and  $X_3$  exhibit peaks or dips at  $\nu = 1/3, 2/3$ , signifying the formation of correlated phases [Fig. 2(e)].

Prior experiments and theoretical simulations [2,16–21] support that the electron phases at  $\nu = 1/3$  ( $2/3$ ) should correspond to a generalized Wigner crystal phase, in which the electrons occupy  $1/3$  ( $2/3$ ) of the moiré cells to form a triangular (honeycomb) lattice, as illustrated in Fig. 1(e). A recent study by scanning tunneling microscopy (STM) has visualized the  $\nu = 1/3, 2/3$ , and  $1/2$  electron

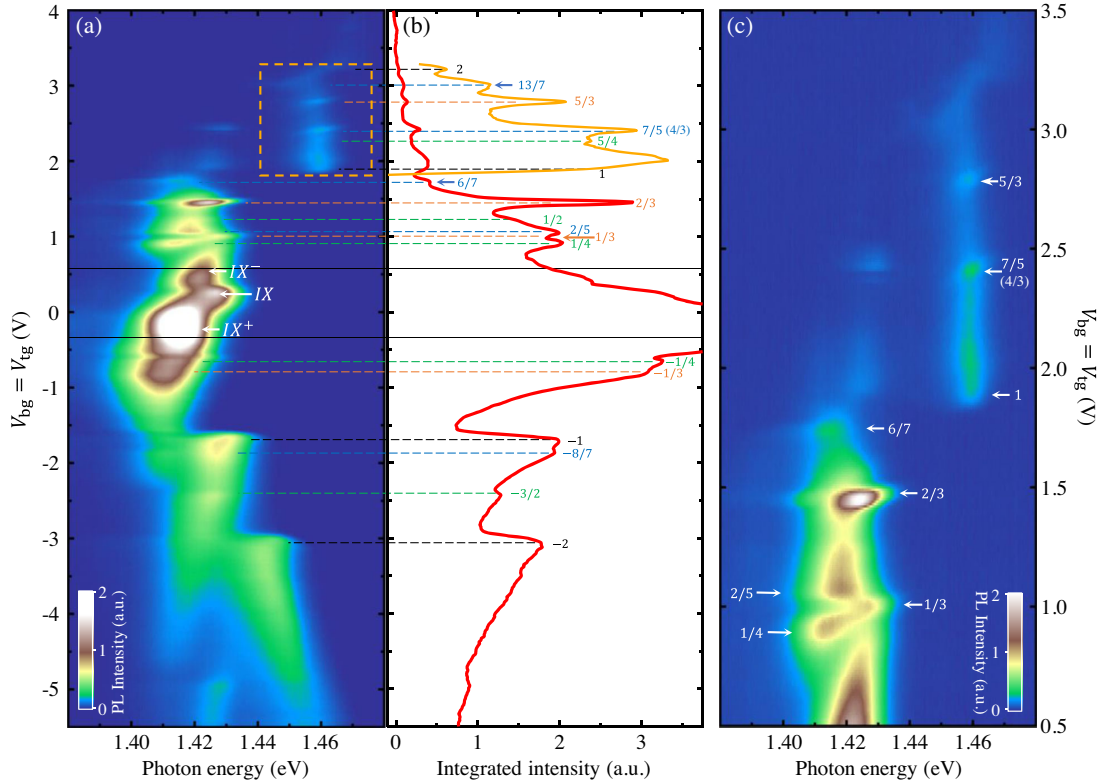


FIG. 3. (a) Gate-dependent PL map for the interlayer excitonic states at  $T \sim 15$  K under 532-nm continuous laser excitation with incident power  $\sim 60$  nW. The PL peak in  $V_g = V_{\text{bg}} = V_{\text{tg}} = 0.2\text{--}0.3$  V corresponds to the interlayer exciton ( $IX$ ); all other PL features should correspond to interlayer trions or exciton-polarons ( $IX^+$ ,  $IX^-$ ). (b) Integrated PL intensity in panel (a) as a function of gate voltage. The red line is the PL intensity integrated over the whole photon energy range in panel (a); the orange line is the PL intensity integrated within the range of the orange dashed box in panel (a). The horizontal dashed lines denote the integer and fractional filling positions. Panels (a) and (b) share the same y axis. (c) Expanded map in  $V_g = 0.5\text{--}3.5$  V in panel (a). The filling factors are denoted. There is some ambiguity in distinguishing  $7/5$  and  $4/3$  states, whose features may overlap in the map.

distributions [39]. In these phases, each electron is locked in its own moiré cell due to the strong Coulomb repulsion between electrons, resulting in insulating phases with no free carriers. The insulating phases with reduced charge screening can renormalize the band gap and exciton binding. Therefore, we expect a modulation of the exciton oscillator strength and resonance energy, which is manifested as peaks or dips in the gate-dependent conductivity profile, as observed in our experiment.

In our results, the fractional correlated phases modulate the higher-lying moiré excitons more strongly than the lower-lying moiré excitons. As we examine their conductivity modulation at  $\nu = 1/3, 2/3$  in Fig. 2(e), the percentage change of conductivity is the largest for  $X_3$  ( $\sim 29\%$ ), smaller for  $X_2$  ( $\sim 6\%$ ), and the smallest for  $X_1$  ( $\sim 1.8\%$ ). The different modulation can be qualitatively understood by two considerations. First, the higher-lying moiré excitons have spatially more extended wave functions than the lower-lying moiré excitons, as shown by prior research [24]; hence the higher-lying states are more sensitive to the larger-period generalized Wigner crystal structure. Second, in our  $\text{WS}_2/\text{WSe}_2$  heterobilayer system,  $X_1$  mainly comes from the original  $A$  exciton in monolayer  $\text{WSe}_2$ , whereas  $X_2$  and  $X_3$  are generated entirely by the relatively weak superlattice effect [2]; hence  $X_1$  has a larger oscillator strength and is more robust against the perturbation of the generalized Wigner crystals than  $X_2$  and  $X_3$ . Therefore, it is reasonable that the generalized Wigner crystals have a larger percentage impact on  $X_2$  and  $X_3$  than on  $X_1$ .

We have also observed substantial changes of the emission spectra at fractional fillings. Figure 3(a) displays a gate-dependent PL map of the interlayer excitonic states in the  $\text{WSe}_2/\text{WS}_2$  heterobilayer. The map shows the emission from the interlayer excitons ( $IX$ ) and interlayer trions (or exciton polarons) on the electron side ( $IX^-$ ) and hole side ( $IX^+$ ) [Fig. 3(a)]. The most prominent features in the map are the drastic steplike jump of emission photon energy and intensity at  $\nu = -1, -2$  on the hole side. To reveal the fine features, we plot the gate-dependent integrated PL intensity in Fig. 3(b). We observe PL enhancement at  $\nu = -1/4, -1/3, -8/7, -3/2$  on the hole side.

The interlayer trions also exhibit PL enhancement at  $\nu = 1, 2$  on the electron side. Compared to the hole side, the trions exhibit many more fractional correlated states on the electron side [Figs. 3(a)–3(b)]. To show the fine features on the electron side, Fig. 3(c) displays an expanded map at  $V_g = V_{\text{bg}} = V_{\text{tg}} = 0.5\text{--}3.5$  V, in addition to the gate-dependent integrated PL intensity profiles in Fig. 3(b). From the trion PL energy and intensity modulation, we can identify correlated phases at many fractional fillings, including  $\nu = 1/4, 1/3, 2/5, 2/3, 6/7, 5/4, 5/3, 13/7$  (Fig. S1 [33]). Similar PL maps are also observed at different positions of our device (Fig. S2 [33]). Our assigned filling factors are mostly consistent with other studies [16,18], including recent PL results from another group [17].

The numerous fractional fillings imply the existence of many correlated electronic phases with different charge orders in the moiré superlattice. Figure 1(e) illustrates some possible charge-order configurations for  $\nu = 1/2, 2/5, 1/3, 1/4, 1/7$  and the complementary  $1-\nu$  fillings. In these phases, the electrons are locked in their own moiré cells to form a periodic structure so as to minimize their interaction potential energy. Since such crystalline electron phases are insulating, they can modulate the band gap and trion binding. Moreover, when a localized electron in the crystalline phase is bound with an exciton to form a trion, the trion state should also be localized in a moiré cell. Such localization may also modulate the trion emission energy.

We have measured the reflectance contrast and PL maps at different temperatures (Figs. S3, S4 [33]). The fractional filling features in both reflection and PL appear to subside at  $T > 30$  K. But the  $\nu = -2$  feature, which corresponds to the full filling of a miniband, can sustain up to  $T \sim 75$  K. The  $|\nu| = 1$  features, which correspond to the Mott or charge-transfer phases, can sustain to  $T > 150$  K. These results, consistent with prior research [2,3,16,18], indicate that the Mott or charge-transfer gap is larger than the miniband energy gap, and the miniband gap is larger than the energy gap of the fractional correlated phases.

Excitonic states in TMD monolayers and moiré superlattices may exhibit valley polarization, signified by circularly polarized luminescence [32,40–46]. It is interesting

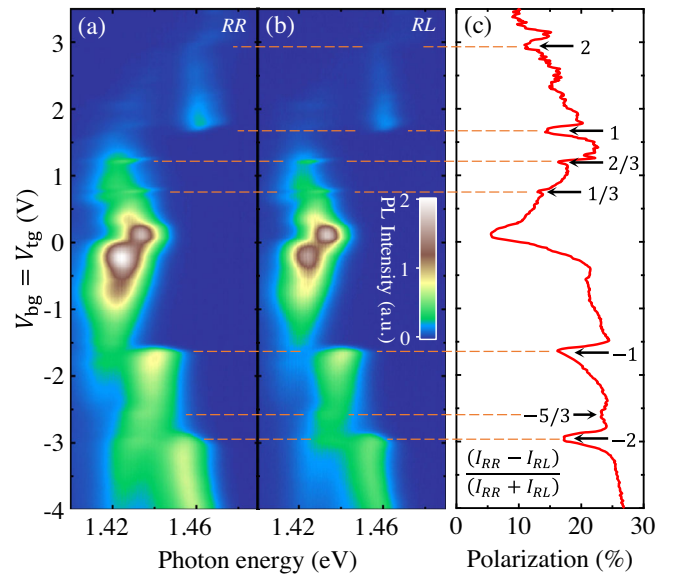


FIG. 4. (a) Gate-dependent PL map for the interlayer excitonic states under right-handed (R) circularly polarized optical excitation and detection (RR). (b) Similar map as panel (a) under right-handed (R) optical excitation and left-handed (L) optical detection (RL). (c) Gate-dependent valley polarization. We denote integer and fractional fillings and the charge neutrality point (CNP) with reduced valley polarization. The PL measurements were conducted at  $T \sim 15$  K with 632.8-nm continuous laser excitation at incident power  $\sim 300$  nW.

to study the effect of correlated phases on valley polarization. Figures 4(a) and 4(b) display the right-handed ( $R$ ) and left-handed ( $L$ ) PL maps of the interlayer excitonic states under right-handed 632.8-nm laser excitation. From the spectrally integrated PL intensity ( $I$ ) at the  $R$ - $R$  and  $R$ - $L$  excitation-detection circular polarization configurations, we obtain the valley polarization as  $\eta = (I_{RR} - I_{RL}) / (I_{RR} + I_{RL})$ . The gate-dependent valley polarization exhibits the deepest dip at the charge neutrality point (CNP), moderate dips at integer fillings  $\nu = \pm 1, \pm 2$ , and small dips at fractional fillings  $\nu = -5/3, 1/3, 2/3$  [Fig. 4(c)]. This phenomenon can be qualitatively understood from the different energy gaps and insulation strength of these states. The valley polarization is limited by intervalley scattering, which is contributed by electron-hole exchange interaction. When the heterobilayer transits from conducting to insulating state, the reduction of screening effect will enhance the Coulomb exchange interaction, hence facilitate the intervalley scattering and reduce the valley polarization [43,46]. As the energy gap and insulation strength are the largest at the CNP, smaller at integer fillings, and even smaller at fractional fillings, the degree of valley polarization reduction decreases correspondingly from the CNP to integer and fractional fillings, as observed in our experiment.

In summary, our experiments demonstrate significant modulation of absorption, emission and valley polarization of excitonic states at fractional fillings in a  $\text{WSe}_2/\text{WS}_2$  moiré superlattice. Similar phenomena are expected in other types of moiré superlattices. Our results motivate further exploration of novel excitonic and valleytronic phenomena in the regime of electron crystallization in moiré materials.

We thank Matthew Wilson for assistance in device fabrication and proofreading the manuscript, and thank Yia-Chung Chang and Kin Fai Mak for discussion. C. H. L. acknowledges support from the National Science Foundation (NSF) Division of Materials Research CAREER Grant No. 1945660. Y.-T. C. acknowledges support from NSF under Grant No. DMR-2004701. N. M. G. acknowledges support from NSF Division of Materials Research CAREER Grant No. 1651247 and from the Army Research Office Electronics Division Grant No. W911NF2110260. K. W. and T. T. acknowledge support from the Elemental Strategy Initiative conducted by the MEXT, Japan and the CREST (JPMJCR15F3), JST.

\*Corresponding author.

joshua.lui@ucr.edu

- [1] Y. Cao, V. Fatemi, A. Demir, S. Fang, S. L. Tomarken, J. Y. Luo, J. D. Sanchez-Yamagishi, K. Watanabe, T. Taniguchi, E. Kaxiras, R. C. Ashoori, and P. Jarillo-Herrero, Correlated insulator behaviour at half-filling in magic-angle graphene superlattices, *Nature (London)* **556**, 80 (2018).
- [2] E. C. Regan, D. Wang, C. Jin, M. I. Bakti Utama, B. Gao, X. Wei, S. Zhao, W. Zhao, Z. Zhang, K. Yumigeta, M. Blei, J. D. Carlström, K. Watanabe, T. Taniguchi, S. Tongay, M. Crommie, A. Zettl, and F. Wang, Mott and generalized Wigner crystal states in  $\text{WSe}_2/\text{WS}_2$  moiré superlattices, *Nature (London)* **579**, 359 (2020).
- [3] Y. Tang, L. Li, T. Li, Y. Xu, S. Liu, K. Barmak, K. Watanabe, T. Taniguchi, A. H. MacDonald, J. Shan, and K. F. Mak, Simulation of Hubbard model physics in  $\text{WSe}_2/\text{WS}_2$  Moiré superlattices, *Nature (London)* **579**, 353 (2020).
- [4] Y. Shimazaki, I. Schwartz, K. Watanabe, T. Taniguchi, M. Kroner, and A. Imamoğlu, Strongly correlated electrons and hybrid excitons in a moiré heterostructure, *Nature (London)* **580**, 472 (2020).
- [5] Y. Cao, V. Fatemi, S. Fang, K. Watanabe, T. Taniguchi, E. Kaxiras, and P. Jarillo-Herrero, Unconventional superconductivity in magic-angle graphene superlattices, *Nature (London)* **556**, 43 (2018).
- [6] R. Bistritzer and A. H. MacDonald, Moiré bands in twisted double-layer graphene, *Proc. Natl. Acad. Sci. U.S.A.* **108**, 12233 (2011).
- [7] A. L. Sharpe, E. J. Fox, A. W. Barnard, J. Finney, K. Watanabe, T. Taniguchi, M. A. Kastner, and D. Goldhaber-Gordon, Emergent ferromagnetism near three-quarters filling in twisted bilayer graphene, *Science* **365**, 605 (2019).
- [8] M. Yankowitz, S. Chen, H. Polshyn, Y. Zhang, K. Watanabe, T. Taniguchi, D. Graf, A. F. Young, and C. R. Dean, Tuning superconductivity in twisted bilayer graphene, *Science* **363**, 1059 (2019).
- [9] M. Serlin, C. L. Tschirhart, H. Polshyn, Y. Zhang, J. Zhu, K. Watanabe, T. Taniguchi, L. Balents, and A. F. Young, Intrinsic quantized anomalous Hall effect in a moiré heterostructure, *Science* **367**, 900 (2020).
- [10] X. Lu, P. Stepanov, W. Yang, M. Xie, M. A. Aamir, I. Das, C. Urgell, K. Watanabe, T. Taniguchi, G. Zhang, A. Bachtold, A. H. MacDonald, and D. K. Efetov, Superconductors, orbital magnets and correlated states in magic-angle bilayer graphene, *Nature (London)* **574**, 653 (2019).
- [11] G. Chen, L. Jiang, S. Wu, B. Lyu, H. Li, B. L. Chittari, K. Watanabe, T. Taniguchi, Z. Shi, J. Jung, Y. Zhang, and F. Wang, Evidence of a gate-tunable Mott insulator in a trilayer graphene moiré superlattice, *Nat. Phys.* **15**, 237 (2019).
- [12] G. Chen, A. L. Sharpe, P. Gallagher, I. T. Rosen, E. J. Fox, L. Jiang, B. Lyu, H. Li, K. Watanabe, T. Taniguchi, J. Jung, Z. Shi, D. Goldhaber-Gordon, Y. Zhang, and F. Wang, Signatures of tunable superconductivity in a trilayer graphene moiré superlattice, *Nature (London)* **572**, 215 (2019).
- [13] G. Chen, A. L. Sharpe, E. J. Fox, Y.-H. Zhang, S. Wang, L. Jiang, B. Lyu, H. Li, K. Watanabe, T. Taniguchi, Z. Shi, T. Senthil, D. Goldhaber-Gordon, Y. Zhang, and F. Wang, Tunable correlated Chern insulator and ferromagnetism in a moiré superlattice, *Nature (London)* **579**, 56 (2020).
- [14] L. Wang, E.-M. Shih, A. Ghiotto, L. Xian, D. A. Rhodes, C. Tan, M. Claassen, D. M. Kennes, Y. Bai, B. Kim, K. Watanabe, T. Taniguchi, X. Zhu, J. Hone, A. Rubio, A. N. Pasupathy, and C. R. Dean, Correlated electronic phases in twisted bilayer transition metal dichalcogenides, *Nat. Mater.* **19**, 861 (2020).
- [15] E. Y. Andrei and A. H. MacDonald, Graphene bilayers with a twist, *Nat. Mater.* **19**, 1265 (2020).
- [16] Y. Xu, S. Liu, D. A. Rhodes, K. Watanabe, T. Taniguchi, J. Hone, V. Elser, K. F. Mak, and J. Shan, Correlated insulating

- states at fractional fillings of moiré superlattices, *Nature (London)* **587**, 214 (2020).
- [17] C. Jin, Z. Tao, T. Li, Y. Xu, Y. Tang, J. Zhu, S. Liu, K. Watanabe, T. Taniguchi, J. C. Hone, L. Fu, J. Shan, and K. F. Mak, Stripe phases in  $\text{WSe}_2/\text{WS}_2$  Moiré superlattices, *Nat. Mater.* (2021), <https://doi.org/10.1038/s41563-021-00959-8>.
- [18] X. Huang, T. Wang, S. Miao, C. Wang, Z. Li, Z. Lian, T. Taniguchi, K. Watanabe, S. Okamoto, D. Xiao, S.-F. Shi, and Y.-T. Cui, Correlated insulating states at fractional fillings of the  $\text{WS}_2/\text{WSe}_2$  Moiré lattice, *Nat. Phys.* **17**, 715 (2021).
- [19] Z. Chu, E. C. Regan, X. Ma, D. Wang, Z. Xu, M. I. B. Utama, K. Yumigeta, M. Blei, K. Watanabe, T. Taniguchi, S. Tongay, F. Wang, and K. Lai, Nanoscale Conductivity Imaging of Correlated Electronic States in  $\text{WSe}_2/\text{WS}_2$  Moiré Superlattices, *Phys. Rev. Lett.* **125**, 186803 (2020).
- [20] Y. Zhang, T. Liu, and L. Fu, Electronic structures, charge transfer, and charge order in twisted transition metal dichalcogenide bilayers, *Phys. Rev. B* **103**, 155142 (2021).
- [21] B. Padhi, R. Chitra, and P. W. Phillips, Generalized Wigner crystallization in Moiré materials, *Phys. Rev. B* **103**, 125146 (2021).
- [22] F. Wu, T. Lovorn, E. Tutuc, and A. H. MacDonald, Hubbard Model Physics in Transition Metal Dichalcogenide Moiré Bands, *Phys. Rev. Lett.* **121**, 026402 (2018).
- [23] E. M. Alexeev, D. A. Ruiz-Tijerina, M. Danovich, M. J. Hamer, D. J. Terry, P. K. Nayak, S. Ahn, S. Pak, J. Lee, J. I. Sohn, M. R. Molas, M. Koperski, K. Watanabe, T. Taniguchi, K. S. Novoselov, R. V. Gorbachev, H. S. Shin, V. I. Fal'ko, and A. I. Tartakovskii, Resonantly hybridized excitons in moiré superlattices in van der Waals heterostructures, *Nature (London)* **567**, 81 (2019).
- [24] C. Jin, E. C. Regan, A. Yan, M. Iqbal Bakti Utama, D. Wang, S. Zhao, Y. Qin, S. Yang, Z. Zheng, S. Shi, K. Watanabe, T. Taniguchi, S. Tongay, A. Zettl, and F. Wang, Observation of Moiré excitons in  $\text{WSe}_2/\text{WS}_2$  heterostructure superlattices, *Nature (London)* **567**, 76 (2019).
- [25] K. Tran *et al.*, Evidence for Moiré excitons in van der Waals heterostructures, *Nature (London)* **567**, 71 (2019).
- [26] X. Lu, X. Li, and L. Yang, Modulated interlayer exciton properties in a two-dimensional Moiré crystal, *Phys. Rev. B* **100**, 155416 (2019).
- [27] D. A. Ruiz-Tijerina and V. I. Fal'ko, Interlayer hybridization and Moiré superlattice minibands for electrons and excitons in heterobilayers of transition-metal dichalcogenides, *Phys. Rev. B* **99**, 125424 (2019).
- [28] C. Jin, E. C. Regan, D. Wang, M. Iqbal Bakti Utama, C.-S. Yang, J. Cain, Y. Qin, Y. Shen, Z. Zheng, K. Watanabe, T. Taniguchi, S. Tongay, A. Zettl, and F. Wang, Identification of spin, valley and Moiré quasi-angular momentum of interlayer excitons, *Nat. Phys.* **15**, 1140 (2019).
- [29] Y. Tang, J. Gu, S. Liu, K. Watanabe, T. Taniguchi, J. Hone, K. F. Mak, and J. Shan, Tuning layer-hybridized Moiré excitons by the quantum-confined Stark effect, *Nat. Nanotechnol.* **16**, 52 (2021).
- [30] Y. Bai, L. Zhou, J. Wang, W. Wu, L. J. McGilly, D. Halbertal, C. F. B. Lo, F. Liu, J. Ardelean, P. Rivera, N. R. Finney, X.-C. Yang, D. N. Basov, W. Yao, X. Xu, J. Hone, A. N. Pasupathy, and X. Y. Zhu, Excitons in strain-induced one-dimensional Moiré potentials at transition metal dichalcogenide heterojunctions, *Nat. Mater.* **19**, 1068 (2020).
- [31] H. Baek, M. Brotons-Gisbert, Z. X. Koong, A. Campbell, M. Rambach, K. Watanabe, T. Taniguchi, and B. D. Gerardot, Highly energy-tunable quantum light from Moiré-trapped excitons, *Sci. Adv.* **6**, eaba8526 (2020).
- [32] K. L. Seyler, P. Rivera, H. Yu, N. P. Wilson, E. L. Ray, D. G. Mandrus, J. Yan, W. Yao, and X. Xu, Signatures of Moiré-trapped valley excitons in  $\text{MoSe}_2/\text{WSe}_2$  heterobilayers, *Nature (London)* **567**, 66 (2019).
- [33] See Supplemental Material at <http://link.aps.org/supplemental/10.1103/PhysRevLett.127.037402>, which includes a detailed description of experimental conditions, additional data, and Refs. [34–37].
- [34] E. Hecht, *Optics*, 3rd ed.(Addison-Wesley, New York, 1998).
- [35] J. W. Weber, V. E. Calado, and M. C. M. v. d. Sanden, Optical constants of graphene measured by spectroscopic ellipsometry, *Appl. Phys. Lett.* **97**, 091904 (2010).
- [36] A. B. Kuzmenko, Kramers–Kronig constrained variational analysis of optical spectra, *Rev. Sci. Instrum.* **76**, 083108 (2005).
- [37] E. Liu, J. van Baren, T. Taniguchi, K. Watanabe, Y.-C. Chang, and C. H. Lui, Landau-Quantized Excitonic Absorption and Luminescence in a Monolayer Valley Semiconductor, *Phys. Rev. Lett.* **124**, 097401 (2020).
- [38] Y. Zhang, N. F. Q. Yuan, and L. Fu, Moiré quantum chemistry: Charge transfer in transition metal dichalcogenide superlattices, *Phys. Rev. B* **102**, 201115(R) (2020).
- [39] H. Li, S. Li, E. Regan, D. Wang, W. Zhao, S. Kahn, K. Yumigeta, M. Blei, T. Taniguchi, K. Watanabe, S. Tongay, A. Zettl, M. Crommie, and F. Wang, Imaging generalized Wigner crystal states in a  $\text{WSe}_2/\text{WS}_2$  Moiré superlattice, preprint available at research square, <https://doi.org/10.21203/rs.3.rs-390032/v1>.
- [40] T. Cao, G. Wang, W. Han, H. Ye, C. Zhu, J. Shi, Q. Niu, P. Tan, E. Wang, B. Liu, and J. Feng, Valley-selective circular dichroism of monolayer molybdenum disulphide, *Nat. Commun.* **3**, 887 (2012).
- [41] K. F. Mak, K. He, J. Shan, and T. F. Heinz, Control of valley polarization in monolayer  $\text{MoS}_2$  by optical helicity, *Nat. Nanotechnol.* **7**, 494 (2012).
- [42] H. Zeng, J. Dai, W. Yao, D. Xiao, and X. Cui, Valley polarization in  $\text{MoS}_2$  monolayers by optical pumping, *Nat. Nanotechnol.* **7**, 490 (2012).
- [43] J. R. Schaibley, H. Yu, G. Clark, P. Rivera, J. S. Ross, K. L. Seyler, W. Yao, and X. Xu, Valleytronics in 2D materials, *Nat. Rev. Mater.* **1**, 16055 (2016).
- [44] G. Wang, A. Chernikov, M. M. Glazov, T. F. Heinz, X. Marie, T. Amand, and B. Urbaszek, Colloquium: Excitons in atomically thin transition metal dichalcogenides, *Rev. Mod. Phys.* **90**, 021001 (2018).
- [45] X. Xu, W. Yao, D. Xiao, and T. F. Heinz, Spin and pseudospins in layered transition metal dichalcogenides, *Nat. Phys.* **10**, 343 (2014).
- [46] H. Yu, X. Cui, X. Xu, and W. Yao, Valley excitons in two-dimensional semiconductors, *Natl. Sci. Rev.* **2**, 57 (2015).